Neuropsychopharmacology www.nature.com/npp

COMMENT OPEN

A versatile GPCR toolkit to track in vivo neuromodulation: not a one-size-fits-all sensor

Marie A. Labouesse[1,2,3] and Tommaso Patriarchi[3,4]

Neuropsychopharmacology (2021) 46:2043–2047; https://doi.org/10.1038/s41386-021-00982-y

A VERSATILE TOOLKIT OF GPCR-SENSORS TO TRACK NEUROMODULATION

Measuring the real-time dynamics of neuromodulator release in the brain with subcellular resolution is a long-sought goal in neuroscience, due to the immense implications for basic science and medicine. The past 3 years have brought this goal within reach, with the appearance of a new class of genetically encoded fluorescent sensors for neuromodulators [1–11] (Fig. 1) constructed using G-protein-coupled-receptors (GPCR) [12]. GPCR sensor design takes advantage of the fact that most neuromodulators harbor GPCRs as their native receptors, and builds on protein engineering expertise acquired through work on genetically encoded calcium sensors [13–16]. High-throughput screening techniques are used to incorporate circularly permuted fluorescent proteins (cpFP) within GPCRs of interest, enabling the optical visualization of neuromodulator dynamics [17]. Given the diversity of naturally existing GPCR scaffolds, there is a large realm of opportunities to generate new GPCR-sensors with tailored properties adapted for each neuromodulator. The dLight1 family exemplifies this possibility, providing a panoply of eight sensors engineered using DRD1, DRD2, and DRD4 receptor subtypes, each with different properties [18]. The rapid developments in GPCR sensor engineering are now allowing an ever-growing ability to tailor sensor use to specific experimental applications, but may create a dilemma for end-users pondering which sensor is best suited for their work or how to interpret results.

TO THE NEUROSCIENTIST END-USER: SENSOR CHOICE RECIPE IN 6 KEY STEPS

Here we provide a step-by-step recipe for end-users (Fig. 1, Supplementary Table S1) to guide sensor choice:

Expected effect size of the experimental manipulation

A sensor's dynamic range (dFF_{max}) (~50% to ~1000%) provides an estimate of the range of responses that can be obtained against varying neuromodulator concentrations. Sensors with good dFF_{max} (which we consider >250%) are always preferable, but particularly when the experiment's effect size (=magnitude of changes in neuromodulator levels, normalized to the standard deviation [19]) is expected to be low (e.g. when measuring changes in tonic release, release in regions with low neuromodulator innervation, or to identify small, dose–response changes in release).

Expected neuromodulator levels in brain region of interest

Existing GPCR-sensors harbor apparent affinities (K_d) ranging from 4 nM up to 7 µM, providing a broad range of detection windows that should be matched to the expected local neuromodulator levels. Indeed, the affinity-based model for receptor–ligand (R–L) interactions [20] posits that, at equilibrium, the fractional occupancy of receptors f depends on the ligand concentration [L] and the receptor's apparent affinity K_d: $f = [L]/(K_d + [L])$. Extending this model to GPCR-sensors, one can predict that sensors should work best when half of the sensors are occupied ($f = 50\%$), i.e. when ligand concentrations [L] are close to the K_d. For example, a medium affinity sensor for DA (e.g. $K_d = 500$ nM) is poorly occupied ($f = 4\%$) at [DA] = 20 nM and thus may not reliably detect tonic DA changes or phasic DA release in regions poorly innervated by DA projections, but should work well in the 100–1000 nM window (~phasic DA in striatum [21, 22]), and only saturate at high (micromolar) concentrations. High-affinity variants (<200 nM) are likely well-suited for capturing tonic release or for regions with low DA innervation (e.g. cortex) but have an elevated risk for ligand buffering (see below). Medium affinity variants with excellent dynamic range ($dFF_{max} \gg 500\%$) may represent a good alternative to increase the breadth of the detection range (higher dFF change for the same change in sensor occupancy). Importantly, in brain regions where multiple neuromodulators of similar structure are released, it is essential to favor sensors with high molecular selectivity, e.g. when tracking DA over NE ($K_{d\text{-}DA} \gg K_{d\text{-}NE}$) [11].

Kinetics of the experimental variables

Sensor on/off-kinetics are highly variable (τ-on: 10 ms–2 s; τ-off: 100 ms–20 s) and should be interpreted with caution (see below). Fast kinetics are generally preferred to track endogenous release dynamics as closely as possible, especially when high temporal resolution is required, e.g. to track the response to closely related events (e.g. cues, optogenetic stimulation) or rapid changes in behavior. In particular, fast on-kinetics will increase sensor responses to brief release events, boosting sensitivity. Fast off-kinetics will also reduce the chance of ligand buffering (τ-off inversely proportional to the dissociation rate constant k_{off} [22]). Slow off-kinetics on the other hand, will integrate temporally close release events resulting in a large global response at the cost of

[1]Department of Psychiatry, College of Physicians and Surgeons, Columbia University, Columbia, NY, USA; [2]Division of Molecular Therapeutics, New York State Psychiatric Institute, New York, NY, USA; [3]Institute of Pharmacology and Toxicology, University of Zurich, Zurich, Switzerland and [4]Neuroscience Center Zurich, University and ETH Zurich, Zurich, Switzerland
Correspondence: Tommaso Patriarchi (patriarchi@pharma.uzh.ch)

Received: 27 October 2020 Revised: 12 January 2021 Accepted: 23 January 2021
Published online: 18 February 2021

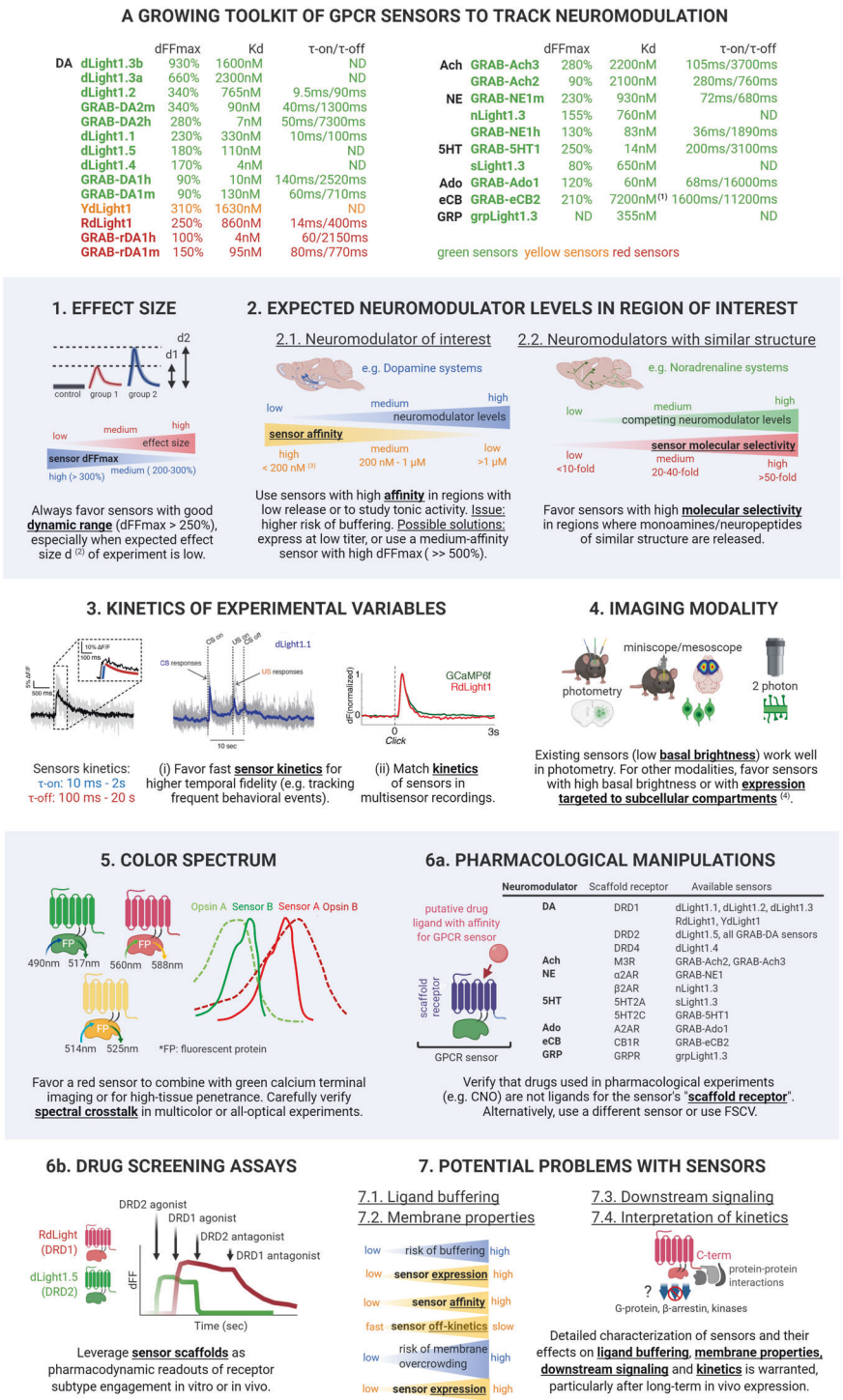

Fig. 1 Choosing a neuromodulator GPCR sensor, a balancing act (see main text for details). (1) K_d for 2AG (reported K_d for AEA: 500 nM [10]). (2) Effect size (*d*1, *d*2): magnitude of change in neuromodulator levels between groups, estimated e.g. by calculating Cohen's *d*: delta of the means of the groups, normalized to the pooled standard deviation [19]. (3) "High" and "low" affinity denominations are relative (here chosen based on DA/NE systems) and may be shifted for other neuromodulators. (4) Expected future developments. 5HT serotonin, Ach acetylcholine, Ado adenosine, CNO clozapine-N-oxide, C-term C-terminal, DA dopamine, DRD1/DRD2 DA receptor 1 and 2, dFFmax dynamic range (maximal dFF), eCB endocannabinoid, FP fluorescent protein, FSCV fast-scan cyclic voltammetry, GRP gastrin-like peptide, K_d apparent affinity, ND not determined, NE noradrenaline, τ-on/τ-off on- and off-sensor kinetics (half-rise, decay times).

temporal detection accuracy, akin to GCaMP6s/7 s ("slow"). Fast kinetics are less critical when tracking average release across hours/days, or when measuring the release of certain slow-acting (minutes) neuropeptides, e.g. gastrin-like peptide [11].

Imaging modality

Existing GPCR-sensors are optimized for fiber photometry given their low basal brightness and relatively high evoked fluorescence. Future sensor variants with higher basal brightness, improved

evoked fluorescence and/or subcellular targeting to individual compartments (e.g. soma vs. dendrites) will be necessary to allow identification and tracking cellular or subcellular release events under miniscope or 2-photon modalities.

Multicolor experiments
GPCR-sensors are compatible with 2-color imaging (e.g. with calcium indicators [1, 2, 4, 10]). If available, red neuromodulator sensors [2, 4] are advantageous in combination with green axon terminal calcium imaging (red terminal imaging is very sensitive to bleaching). Red sensors also offer higher tissue penetrance; which should produce higher SNR in photometry or increase 2-photon maximal imaging depth. GPCR-sensors can also be implemented in all-optical experiments using optogenetic manipulations [1, 2, 4, 7, 10] at orthogonal wavelengths (see refs. [1, 23]). There is a distinct risk for spectral crosstalk between opsin and sensor which should always be tested for by using appropriate controls (see ref. [24]).

Pharmacological considerations
GPCR-sensors are engineered using human neuromodulator receptors and thus can respond to pharmacological ligands. This provides a useful tool to validate neuromodulator sensors using antagonists (see refs. [1, 23]), but also means GPCR-sensors are incompatible with certain pharmacological manipulations. In such cases, sensors responsive to the drug of interest should be avoided in favor of sensors built on a different receptor subtype, or alternatively one can use periplasmic-binding-protein (PBP) sensors [25] or fast-scan cyclic voltammetry (FSCV).

TO THE DRUG HUNTER: A FUTURE WITH RECEPTOR-SUBTYPE SENSOR FAMILIES FOR DRUG SCREENING?

The pharmacological characteristics of GPCR-sensors also represent a unique opportunity for novel drug discovery assays using multicolor fluorescent technology. We provided proof of concept for this possibility by screening DRD1 and DRD2 ligands against red DRD1 and green DRD2 sensors in vitro [2]. Such assays could presumably be deployed in vivo [1–5, 7] to probe pharmacodynamic target engagement of specific receptor subtypes during behavior following drug administration, with high spatiotemporal resolution and cell specificity.

A CAUTIONARY TALE: POTENTIAL PROBLEMS WITH GPCR-SENSORS

GPCR-sensors have several limitations that end-users should be aware of.

Ligand buffering?
There is a risk for sensors to buffer endogenous ligands, i.e. reducing neuromodulator availability at native receptors and in turn affecting endogenous downstream signaling. We verified in vitro [1] that sensor expression does not affect neuromodulator-induced cAMP signaling. However, whether long-term expression of sensors in the intact brain induces ligand buffering is unknown. To address this, one could measure the impact of sensor expression (at increasing concentrations, i.e. increasing AAV titers) on native neuromodulator dynamics obtained with FSCV or other functional (e.g. PKA or cAMP [26, 27]), physiological (e.g. cell firing properties), neuroanatomical (e.g. inflammatory markers) or behavioral readouts. Mathematical modeling could help estimating the risk of ligand buffering, for example by calculating the quantity [LS] of ligand molecules bound to a sensor (sensor affinity Kd_S) and comparing it to the quantity [LR] of ligand molecules bound to a native receptor (receptor affinity Kd_R). We could then use affinity-based models for receptor–ligand interactions [20, 22] which posit that, for two independent receptor populations S and R of concentrations $Bmax_S$ and $Bmax_R$, specific binding = [LS] + [LR] at equilibrium. Ligand buffering at sensors would equate: $[LS] = Bmax_S \times [L]/(Kd_S + [L])$ and ligand binding at native receptors: $[LR] = Bmax_R \times [L]/Kd_R + [L])$. Although this model has its limitations [22], it can make several predictions: (i) The risk of ligand buffering [LS] increases with sensor concentration $Bmax_S$. At present, the concentration of sensors has not been determined (see next paragraph), and it is therefore not possible to determine whether ligand buffering is a significant phenomenon or not. (ii) The risk of ligand buffering increases inversely with the sensor's Kd_S. Thus, high-affinity sensors (low Kd_S values) should be expressed at concentrations ($Bmax_S$) as low as possible to ensure low risk of buffering: $[LS] \ll [LR]$. Sensors with slow off-kinetics (high τ-off) also increase the risk of buffering since Kd_S is inversely proportional to τ-off [20]. (iii) The impact of ligand buffering on native receptor function will depend on their affinities Kd_R. For example, the reported affinity of DA receptors DRD1 and DRD2 are $Kd_{DRD1} = 1600$ nM and $Kd_{DRD2} = 25$ nM, respectively [28]. In the condition when concentrations of sensors $Bmax_S$ and receptors $Bmax_R$ are equal (=Bmax), at low DA concentrations ([DA] = 20 nM), a high affinity sensor ($Kd_S = 50$ nM) has a high chance of affecting DA binding at DRD2 since binding would be of similar magnitude at the sensor and at the DRD2 receptor: $[DA - S] = 29\% \times Bmax \approx [DA - DRD2] = 45\% \times Bmax$. Since DRD1 is less sensitive to low basal DA (low binding at DRD1: $[DA - DRD1] = 1.2\% \times Bmax$), such high-affinity sensors are less likely to have a buffering effect on this receptor subtype at low [DA]. Upon phasic DA release ([DA] = 200 nM), the same high-affinity sensor ($Kd_S = 50$ nM) will have a lesser effect on DRD2 (DRD2 close to saturation: $[DA - DRD2] = 89\% \times Bmax$) but could strongly impact binding at DRD1 ($[DA - S] = 80\% \times Bmax$ vs. $[DA - DRD1] \gg 11\% \times Bmax$). This illustrates how sensors also need to be carefully chosen based on whether changes in tonic DA release (e.g. DA dips at DRD2 [26]) or phasic release are under study. Of course, it must be noted that (i) the spatiotemporal dynamics of release and reuptake [21, 29] and (ii) the number of sensors expressed near the sites of release and exposed to the neuromodulator will further dictate the kinetics and significance of ligand buffering and would need to be incorporated into mathematical models.

Membrane overcrowding?
GPCR-sensors are expressed at the membrane but lack ligand-induced internalization. Although their turnover is not fully understood, it is possible that their surface levels increase over time, which could lead to membrane overcrowding, and in turn affect membrane properties. Acute in vitro dLight1 expression was estimated ~10-fold higher relative to endogenous GPCRs [30] and this expression level did not affect endogenous GPCR signaling pathways [1]. However, neither the level of sensors expressed in vivo, nor the impact on in vivo membrane physiology (e.g. excitability, oligomerization) or toxicity (e.g. cell death) are known and should be addressed in future work. Sensor concentrations in tissue obtained using increasing AAV titers could be quantified using classical radioligand-binding assays; one could expect values around ~1 pmol/mg protein as shown for striatal transgenic DRD2 [31]. High-resolution estimates of sensor expression in functional compartments (e.g. dendrites) obtained using fluorescent tags [32] could also be useful. This would allow to estimate the quantity of sensors actually trafficked near sites of release and thus susceptible to contribute to (1) the fluorescent signal, (2) membrane overcrowding, and (3) ligand buffering.

Impact on downstream signaling?
Since GPCR are membrane receptors, they interact with cellular proteins to induce downstream signaling. It was verified that GPCR-sensors do not couple with G-protein or beta-arrestin pathways [1, 3]. However, GPCRs, in particular their C-terminus,

are involved in a multitude of other protein–protein interactions, including kinases (e.g. PKA/PKC, GRK) and other scaffold proteins (e.g. PDZ-domain-containing proteins) [33] which should be investigated in future work.

Interpretation of transient kinetics?
Kinetics of obtained data should be interpreted with caution [25]. Ideally, sensor on/off-kinetics primarily reflect the kinetics of exposure (release/clearance) to the neuromodulator. However, they are likely also influenced by the sensor's structure, which impacts kinetics of ligand binding/unbinding and conformational dynamics. For example, since GPCR-sensors do not couple with G-proteins, they likely cannot adopt the "high-affinity" orthosteric state induced by G-protein binding [34]. This may affect ligand binding/unbinding dynamics observed at GPCR-sensors and in turn impact (1) the kinetics of the sensor and therefore also (2) the kinetics of measured transients.

FUNDING AND DISCLOSURE

This work was made possible by funding from the European Research Council (ERC) under the European Union's Horizon 2020 research and innovation program (Grant agreement Nos. 891959 and 101016787) to TP, and Swiss National Science Foundation grants (#P400PB_180841, #P4P4PB_191069) to MAL. We also acknowledge funding from Swiss National Science Foundation (Grant No. 310030_196455), Novartis Foundation for Medical–Biological Research, Olga Mayenfisch Foundation, Hartmann Müller Foundation for Medical Research grants to TP; TP is listed as inventor on a patent application related to the technology described in this article. MAL has nothing to disclose.

ACKNOWLEDGEMENTS

The authors thank C. Kellendonk for infrastructural support. Figures were created with BioRender.com.

AUTHOR CONTRIBUTIONS

MAL and TP wrote the paper and made figures.

FUNDING

Open Access funding provided by Universität Zürich.

ADDITIONAL INFORMATION

Supplementary information The online version contains supplementary material available at https://doi.org/10.1038/s41386-021-00982-y.

Publisher's note Springer Nature remains neutral with regard to jurisdictional claims in published maps and institutional affiliations.

REFERENCES

1. Patriarchi T, Cho JR, Merten K, Howe MW, Marley A, Xiong W-H, et al. Ultrafast neuronal imaging of dopamine dynamics with designed genetically encoded sensors. Science. 2018;360:eaat4422.
2. Patriarchi T, Mohebi A, Sun J, Marley A, Liang R, Dong C, et al. An expanded palette of dopamine sensors for multiplex imaging in vivo. Nat Methods. 2020;17:1147–55.
3. Sun F, Zeng J, Jing M, Zhou J, Feng J, Owen SF, et al. A genetically encoded fluorescent sensor enables rapid and specific detection of dopamine in flies, fish, and mice. Cell 2018;174:481–96.e19.
4. Sun F, Zhou J, Dai B, Qian T, Zeng J, Li X, et al. Next-generation GRAB sensors for monitoring dopaminergic activity in vivo. Nat Methods. 2020;17:1156–66.
5. Jing M, Li Y, Zeng J, Huang P, Skirzewski M, Kljakic O, et al. An optimized acetylcholine sensor for monitoring in vivo cholinergic activity. Nat Methods. 2020;17:1139–46.
6. Oe Y, Wang X, Patriarchi T, Konno A, Ozawa K, Yahagi K, et al. Distinct temporal integration of noradrenaline signaling by astrocytic second messengers during vigilance. Nat Commun. 2020;11:471.
7. Feng J, Zhang C, Lischinsky JE, Jing M, Zhou J, Wang H, et al. A genetically encoded fluorescent sensor for rapid and specific in vivo detection of norepinephrine. Neuron 2019;102:745–61.e8.
8. Peng W, Wu Z, Song K, Zhang S, Li Y, Xu M. Regulation of sleep homeostasis mediator adenosine by basal forebrain glutamatergic neurons. Science. 2020;369:eabb0556.
9. Wan J, Peng W, Li X, Qian T, Song K, Zeng J, et al. A genetically encoded GRAB sensor for measuring serotonin dynamics in vivo. Preprint at *bioRxiv* https://doi.org/10.1101/2020.02.24.962282 (2020).
10. Dong A, He K, Dudok B, Farrell JS, Guan W, Liput DJ, et al. A fluorescent sensor for spatiotemporally resolved endocannabinoid dynamics in vitro and in vivo. Preprint at *bioRxiv* https://doi.org/10.1101/2020.10.08.329169 (2020).
11. Melzer S, Newmark E, Mizuno GO, Hyun M, Philson AC, Quiroli E, et al. Bombesin-like peptide recruits disinhibitory cortical circuits and enhances fear memories. Preprint at *bioRxiv* https://doi.org/10.1101/2020.10.26.355123 (2020).
12. Wacker D, Stevens RC, Roth BL. How ligands illuminate GPCR molecular pharmacology. Cell 2017;170:414–27.
13. Akerboom J, Chen T-W, Wardill TJ, Tian L, Marvin JS, Mutlu S, et al. Optimization of a GCaMP calcium indicator for neural activity imaging. J Neurosci. 2012;32:13819–40.
14. Dana H, Mohar B, Sun Y, Narayan S, Gordus A, Hasseman JP, et al. Sensitive red protein calcium indicators for imaging neural activity. ELife 2016;5:e12727.
15. Tian L, Hires SA, Mao T, Huber D, Chiappe ME, Chalasani SH, et al. Imaging neural activity in worms, flies and mice with improved GCaMP calcium indicators. Nat Methods. 2009;6:875–81.
16. Dana H, Sun Y, Mohar B, Hulse BK, Kerlin AM, Hasseman JP, et al. High-performance calcium sensors for imaging activity in neuronal populations and microcompartments. Nat Methods. 2019;16:649–57.
17. Vardy E, Roth BL. Conformational ensembles in GPCR activation. Cell 2013;152:385–6.
18. Labouesse MA, Cola RB, Patriarchi T. GPCR-based dopamine sensors—a detailed guide to inform sensor choice for in vivo imaging. Int J Mol Sci. 2020;21:8048.
19. Button KS, Ioannidis JPA, Mokrysz C, Nosek BA, Flint J, Robinson ESJ, et al. Power failure: why small sample size undermines the reliability of neuroscience. Nat Rev Neurosci. 2013;14:365–76.
20. Motulsky HJ, Neubig RR. Analyzing binding data. Curr Protoc Neurosci. 2010;52:7.5.1–7.5.65.
21. Sulzer D, Cragg SJ, Rice ME. Striatal dopamine neurotransmission: regulation of release and uptake. Basal Ganglia. 2016;6:123–48.
22. Hunger L, Kumar A, Schmidt R. Abundance compensates kinetics: similar effect of dopamine signals on D1 and D2 receptor populations. J Neurosci. 2020;40:2868–81.
23. Lefevre EM, Pisansky MT, Toddes C, Baruffaldi F, Pravetoni M, Tian L, et al. Interruption of continuous opioid exposure exacerbates drug-evoked adaptations in the mesolimbic dopamine system. Neuropsychopharmacology. 2020. https://doi.org/10.1038/s41386-020-0643-x.
24. Kim CK, Yang SJ, Pichamoorthy N, Young NP, Kauvar I, Jennings JH, et al. Simultaneous fast measurement of circuit dynamics at multiple sites across the mammalian brain. Nat Methods. 2016;13:325–8.
25. Sabatini BL, Tian L. Imaging neurotransmitter and neuromodulator dynamics in vivo with genetically encoded indicators. Neuron 2020;108:17–32.
26. Lee SJ, Lodder B, Chen Y, Patriarchi T, Tian L, Sabatini BL. Cell-type-specific asynchronous modulation of PKA by dopamine in learning. Nature. 2020. https://doi.org/10.1038/s41586-020-03050-5. Epub ahead of print. PMID: 33361810.
27. Harada K, Ito M, Wang X, Tanaka M, Wongso D, Konno A, et al. Red fluorescent protein-based cAMP indicator applicable to optogenetics and in vivo imaging. Sci Rep. 2017;7:7351.
28. Richfield EK, Penney JB, Young AB. Anatomical and affinity state comparisons between dopamine D1 and D2 receptors in the rat central nervous system. Neuroscience 1989;30:767–77.
29. Cragg SJ, Rice ME. DAncing past the DAT at a DA synapse. Trends Neurosci. 2004;27:270–7.
30. Patriarchi T, Cho JR, Merten K, Marley A, Broussard GJ, Liang R, et al. Imaging neuromodulators with high spatiotemporal resolution using genetically encoded indicators. Nat Protoc. 2019;14:3471–505.
31. Gallo EF, Salling MC, Feng B, Morón JA, Harrison NL, Javitch JA, et al. Upregulation of dopamine D2 receptors in the nucleus accumbens indirect pathway increases locomotion but does not reduce alcohol consumption. Neuropsychopharmacology. 2015;40:1609–18.
32. Grimm JB, Muthusamy AK, Liang Y, Brown TA, Lemon WC, Patel R, et al. A general method to fine-tune fluorophores for live-cell and in vivo imaging. Nat Methods. 2017;14:987–94.

33. Bockaert J, Marin P, Dumuis A, Fagni L. The 'magic tail' of G protein-coupled receptors: an anchorage for functional protein networks. FEBS Lett. 2003;546: 65–72.
34. Weis WI, Kobilka BK. The molecular basis of G protein-coupled receptor activation. Annu Rev Biochem. 2018;87:897–919.